

Compliant Electropermanent Magnets

William R. Johnson III¹ and Rebecca Kramer-Bottiglio¹

Abstract—Modular and climbing robots have employed electropermanent magnets as a power-efficient alternative to electromagnets for tasks that involve attaching modules or exerting forces on ferromagnetic surfaces. In this paper, we present compliant electropermanent magnets that extend the benefits of electropermanent magnets to the field of soft robotics. We describe a process for designing compliant electropermanent magnets with different materials and mixing ratios to achieve desired properties without sacrificing the mechanical compliance necessary for integration into soft robots. Finally, we characterize the performance of the compliant electropermanent magnets and demonstrate their ability to repeatedly and reversibly switch their magnetization ON and OFF.

I. INTRODUCTION

The growing field of soft robotics aims to create robots whose mechanical compliance makes them more robust, more versatile, and safer for interacting with humans [1]. Toward this goal, researchers have developed compliant analogues to traditional robot components for sensing [2], [3], actuation [4], and computation [5].

A subset of soft robots leverage electromagnetism for their actuation strategies [6]–[8]. Many researchers embed magnetic particles into silicone elastomers to make soft magnetic composites that can be actuated with external magnetic fields [9]–[12] or local magnetic fields [13], [14]. Kohls *et al.* designed a soft electromagnet with a coil of liquid metal and a soft magnetic composite [15] and then extended this work to produce an all-soft electric motor [16]. Li *et al.* introduced magnetic putty as a reprogrammable, self-healing building material for soft robots [17].

As an alternative to power-hungry electromagnets, roboticians have made use of electropermanent magnets [18]. Electropermanent magnets consist of two permanent magnets with the same magnetization but different coercivities [19]. A conductive coil is wrapped around the magnet such that a brief pulse of current can generate a magnetic field strong enough to reverse the magnetization of the low-coercivity magnet but not strong enough to affect the high-coercivity magnet. Thus, by selectively reversing the polarity of the low-coercivity magnet, the system can be turned ON (nonzero net magnetization) or OFF (neutral net magnetization). In contrast to electromagnets, which continuously draw current, the electropermanent magnet only consumes energy briefly when the state is switched; the permanent magnets do not consume power, even in the ON state [20].

*This work was supported by NASA CT Space Grant under PTE Federal Award No: 80NSSC20M0129. WRJ was supported by the National Science Foundation (NSF) under grant no. IIS-1955225.

¹Dept. of Mechanical Engineering and Materials Science, Yale University, New Haven, CT, USA will.johnson@yale.edu

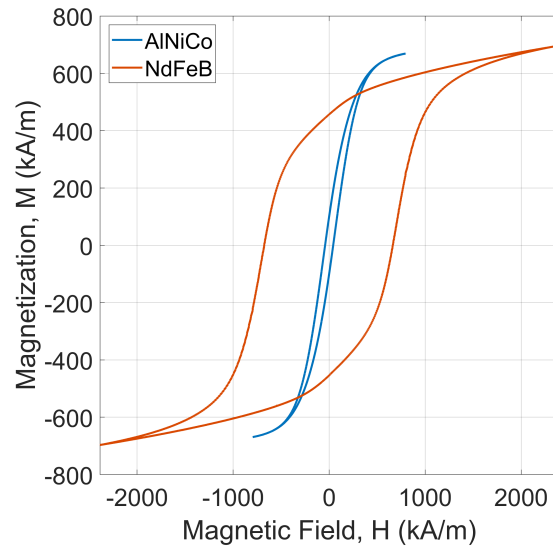


Fig. 1. Magnetic hysteresis curves for AlNiCo and NdFeB samples (one each) at a temperature of 300 K. With a far wider hysteresis loop, NdFeB has a much higher coercivity. The vertical axis intercepts show that NdFeB also has a greater remanent magnetization. Here, the magnetization is normalized by the volume of the magnetic material, not the total volume of the sample.

Electropermanent magnets save energy for applications where the switching frequency between ON and OFF is low [21]. Researchers have chosen electropermanent magnets for modular robots that attach together to complete a task and later detach [22]. Hong *et al.* employed electropermanent magnets for a legged robot that climbs ferromagnetic surfaces [23]. In soft robotics, electropermanent magnets have been used in valves [24], [25] and as actuators [26], but there is still no soft analogue to these rigid electropermanent magnets. Modular soft robots need modular connectors that are strong, energy-efficient, and congruent with their compliant bodies [27]; however, many modular soft robots use rigid magnets [28]–[33], compromising on body compliance, or melting adhesives [34], which consume a large amount of energy. Park *et al.* introduced a soft robot that climbs ferromagnetic surfaces [35], reminiscent of [23], but the robot had to have a partially rigid body to accommodate rigid permanent magnets.

In this paper, we present a compliant electropermanent magnet, a soft analogue to electropermanent magnets previously introduced in the literature. Our experimental characterization provides soft roboticists the data they need to design compliant electropermanent magnets to fit a variety of specifications (e.g., modulus, pull-off force, coercivity,

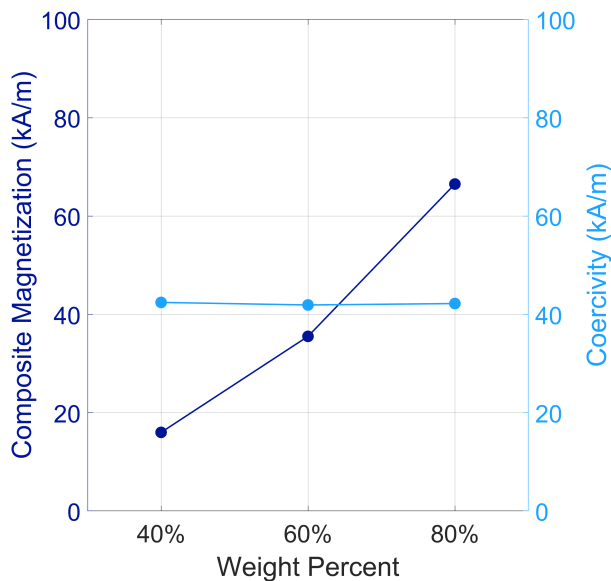


Fig. 2. Coercivity and remanent magnetization for AlNiCo composites at different loading weight percents. Greater weight percents of magnetic powder can lead to greater residual flux densities without changing the coercivity. Here, the composite magnetization is the remanence normalized by the volume of the composite, hence why greater weight percents show greater magnetization (if we normalize by the volume of magnetic material, all three magnetizations are similar). Each data point represents one sample measured on the SQUID-VSM at a temperature of 300 K.

remanent magnetization) for a diversity of applications, including modular connections, climbing robots, and pick and place tasks. After a brief note on nomenclature (Section I-A) and a description of our design process (Section II), we characterize the magnetic and mechanical properties of our compliant magnets in Sections III and IV, respectively. Finally, we demonstrate the compliant electropermanent magnet in Section V.

A. Nomenclature

In soft robotics, the word “soft” commonly refers to materials and structures with low elastic moduli, affording them bulk mechanical compliance [1]. Physicists who study magnetism use the word “soft” to refer to magnetic materials with low coercivity, meaning their polarity can be easily reversed in the presence of weak applied magnetic fields [17]. To eschew confusion, we avoid the word “soft” when possible in the remaining sections of this paper; instead we use “compliant” to refer to a material’s mechanical properties (i.e., low elastic modulus) and “low-coercivity” to refer to a material’s magnetic properties.

II. DESIGN AND FABRICATION

Researchers have built electropermanent magnets using aluminum-nickel-cobalt (AlNiCo) as the low-coercivity magnet and neodymium-iron-boron (NdFeB) as the high-coercivity magnet [18]–[26]. The critical design parameters in selecting these materials are coercivity and remanent magnetization: the two magnets should have similar magnetization but significantly different coercivities. With these parameters, the polarity of the low-coercivity magnet can be

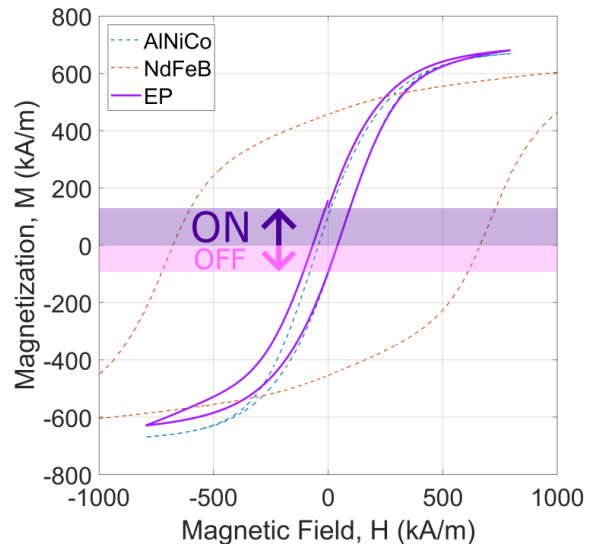


Fig. 3. Magnetic hysteresis curve for the 80% (by weight) EP sample at a temperature of 300 K compared to the curves from Figure 1. The sample was magnetized in a saturating field (2,400 kA/m), and the field was removed immediately before this hysteresis was measured between -800 kA/m and 800 kA/m. The hysteresis loop is no longer symmetric with respect to $M = 0$ but rather shifted up such that the remanent magnetization (at $H = 0$) is larger on the upper part of the curve and smaller on the lower part, meaning the material can be used as an electropermanent magnet. The shaded regions visualize the asymmetry with respect to the horizontal axis. The magnetization is normalized by the volume of the magnetic material.

reversed without affecting the high-coercivity magnet, and when the magnets are oppositely magnetized (the OFF state) there will be no net magnetization.

While previous electropermanent magnets have been assemblies of rigid components, here we present the design of a composite material using AlNiCo powder (AL-NICO-01-P.200M; American Elements) and NdFeB powder (FE-NDB-02R-P.10UM; American Elements) mixed into a silicone elastomer (Eco-Flex 50; Smooth-On). An advantage of this approach, in addition to mechanical compliance, is the ability to tune the properties of the electropermanent magnets by changing the mixing ratios.

Our design process involves first characterizing the magnetic properties of the two magnetic materials, especially coercivity and remanent magnetization (Section III). From these properties, we calculate the *electropermanent (EP) mixing ratio* (by weight) where the AlNiCo and NdFeB parts will have the same remanence. In Section IV, we investigate the trade-offs between mechanical compliance and pull-off force as a function of magnetic powder weight percent. The compositions of the two magnetic powders, which can be used to calculate the weight of an electropermanent magnet, are given in Table I. The average particle size is $\leq 10 \mu\text{m}$ for the NdFeB powder and $\leq 74 \mu\text{m}$ for the AlNiCo powder.

III. VIBRATING SAMPLE MAGNETOMETRY

The magnetic properties of the composite materials were tested with a superconducting quantum interference device (SQUID) magnetometer (MPMS 3; Quantum Design) using

AlNiCo		NdFeB	
Al	10%	Nd	19.1%
Ni	19%	Fe	73.7%
Co	13%	B	0.9%
Fe	58%	Pr	6.3%

TABLE I
COMPOSITION OF MAGNETIC POWDERS BY WEIGHT

vibrating-sample magnetometry (VSM). Samples were prepared by mixing magnetic powder (AlNiCo or NdFeB) with pre-cure silicone (Eco-Flex 50) at a given weight percent and curing the composite in an acrylic mold for four hours at room temperature. This process produced cylindrical samples that were 1.6 mm thick and 1.4 mm in diameter.

The magnetic hysteresis loops for the 80% (by weight) AlNiCo and NdFeB samples, as measured by SQUID-VSM, are shown in Figure 1. The magnetic hysteresis is measured by applying a varying magnetic field H and measuring the magnetic moment of the sample. The vertical axis is the magnetization of the sample, defined as the magnetic moment normalized by volume. Here, we normalize by the volume of the magnetic material, ignoring the volume of the silicone in the composite. The remanent magnetization, the magnetization of the sample in the absence of an applied field, is the vertical axis intercept of the hysteresis curve, and the coercivity, the external field required to reverse the polarity of the sample, is the horizontal intercept. The width of the NdFeB hysteresis loop confirms that its coercivity (676 kA/m) is an order of magnitude greater than the coercivity of AlNiCo (42 kA/m). Moreover, the remanent magnetization of NdFeB (456 kA/m) is greater than that of AlNiCo (100 kA/m) by a factor of 4.55. Therefore, to design electropermanent magnets where the AlNiCo and NdFeB components have the same residual flux density, we need a volume mixing ratio of 4.55:1, which means a mixture of 82.2% AlNiCo and 17.8% NdFeB by weight. We call this mixture EP for electropermanent.

Figure 2 confirms that modifying the weight percent of AlNiCo in the AlNiCo-silicone composite indeed changes the residual flux density without affecting the coercivity. So, an EP sample was prepared that is also 1.6 mm thick and 1.4 mm in diameter, and it is 80% EP by weight (where EP is a mixture that is 82.2% AlNiCo and 17.8% NdFeB by weight). A hysteresis curve for the EP sample is shown in Figure 3 and compared to the curves from Figure 1. The EP sample was first magnetized in a saturating field (2,400 kA/m), and then the field was removed before the hysteresis loop was measured between -800 kA/m and 800 kA/m. The discontinuity on the upper part of the curve at $H = 0$ indicates that the remanent magnetization is lower after one hysteresis cycle (i.e., turning the EP magnet OFF and ON again) since we only apply a field of 800 kA/m instead of returning to the saturating field of $2,400$ kA/m. Compared to Figure 1, the hysteresis curve in Figure 3 is shifted up such that the remanent magnetization (when the applied magnetic field is zero) on the lower part of the curve is closer to zero than the remanent magnetization on the upper part of the curve. This feature of the hysteresis curve

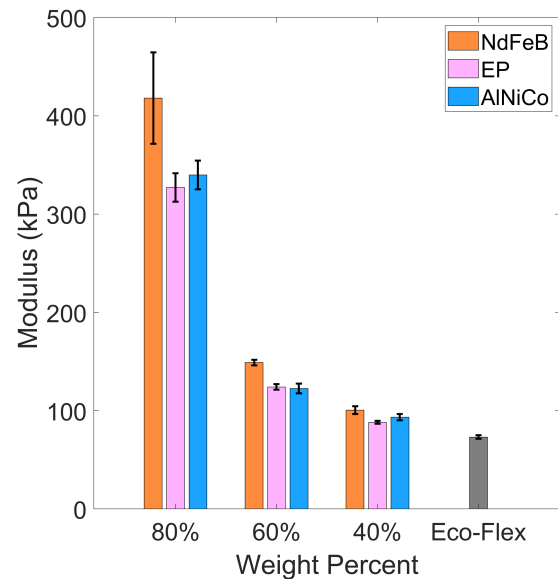
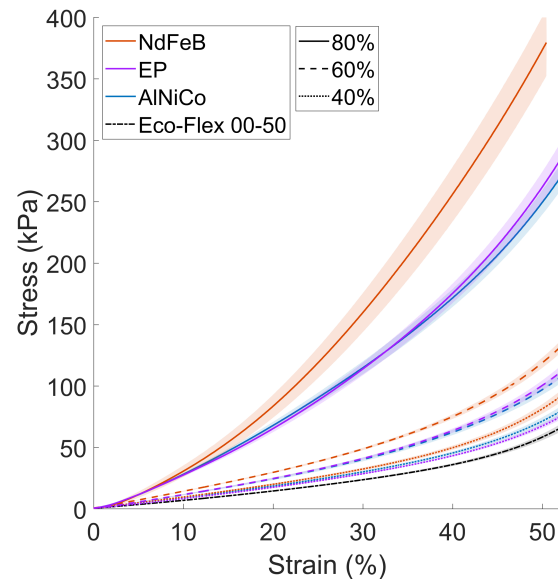


Fig. 4. Compression modulus measurements for samples of varying material and weight percent. (Top) Stress vs. strain curves for magnetic composites compared to neat Eco-Flex 00-50. Solid lines represent the mean of five samples, and shaded areas represent one standard deviation. (Bottom) Compressive modulus for the same samples, calculated for the region $\leq 20\%$ strain. Colored bars represent the mean of five samples while error bars represent one standard deviation. Higher weight percents lead to stiffer materials, and the EP material has a similar stiffness to AlNiCo since it is mostly AlNiCo by weight.

indicates that the material, once magnetized in a saturating field, can easily be switched between a high-remanence ON state and low-remanence OFF state, a desired property for applications like module attachment and climbing robots. Since we were motivated by these applications, we designed the EP mixture to have a remanence close to zero on the lower part of the hysteresis curve, but we note that other mixing ratios could be used for tunable magnetic properties. For example, in applications where a nonzero remanence in the OFF state can be tolerated, a ratio with more NdFeB could be used, shifting the hysteresis loop further upward

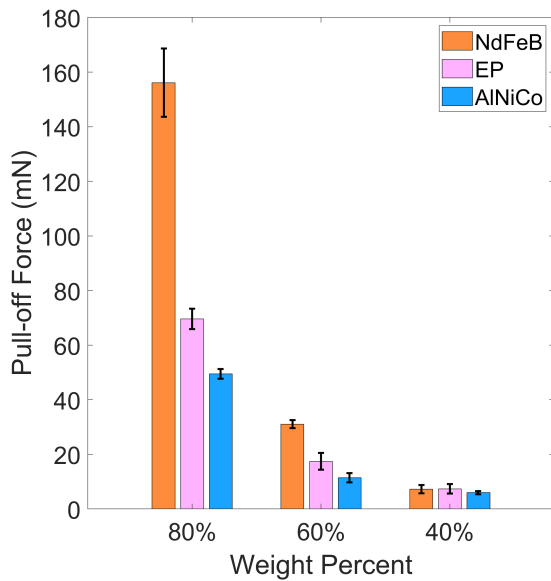


Fig. 5. Magnetic pull-off force of magnetized samples of varying materials and weight percents. Samples were magnetized with a self-contained magnetizer. Then, the maximum pull-off force was measured after compressing samples with a steel plate. The mean of five samples is plotted where error bars indicate the standard deviation. Higher weight percents lead to greater magnetic forces. Congruent with Figure 3, NdFeB is the strongest magnet. The EP mixture compromises on strength in favor of its electropermanence.

and leading to stronger forces in the ON state. For the rest of this paper, the EP samples are prepared with the ratio calculated in this section.

IV. MECHANICAL CHARACTERIZATION

Next, we characterize the mechanical properties of the compliant electropermanent magnets. Similar to Section III, samples were prepared by mixing magnetic powder into pre-cure Eco-Flex 50 at specific weight percents, filling acrylic molds with the composite, and curing for four hours at room temperature. Samples in this section are cylinders with a diameter of 6.35 mm and a height of 6.35 mm. Experiments were conducted on a materials testing system (Instron 3345) with a 50-N load cell (Instron 2519-102; 0.1 mN resolution).

A. Elastic Modulus

Compression tests were conducted to characterize the mechanical compliance of our electropermanent magnets as a function of magnetic powder material and weight percent. Figure 4 shows the results of five samples of each material and weight percent compressed between two acrylic plates, each 6.35 mm thick, at a rate of 3 mm/min. At 80% magnetic powder by weight, samples are stiffer, but on the same order of magnitude as neat Eco-Flex. At lower weight percents, the composites approach the compliance of neat Eco-Flex, but lower weight percents also come with the trade-off of weaker magnetic moments (see Section IV-B). The plots in Figure 4 show data from the same experiments; the compression modulus in the bottom plot is calculated in the region from 0% to 20% strain. The EP and AlNiCo moduli match closely because the EP mixture is mostly AlNiCo by weight; NdFeB composites are stiffer.

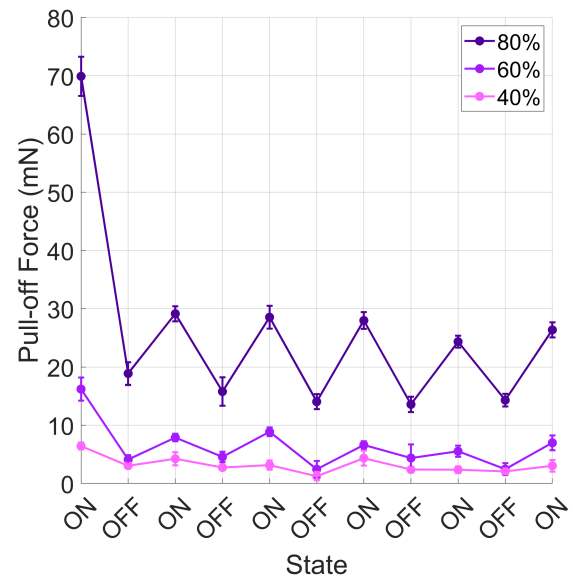


Fig. 6. Magnetic pull-off force of EP samples of varying weight percent after toggling states. The leftmost ON state is immediately after the sample was magnetized. Samples were subsequently switched OFF and ON and measured as in Figure 5. Markers represent the mean of five samples while error bars represent the standard deviation. The EP magnets lose some of their strength, compared to their initial magnetization, when they are first switched OFF and back ON, but thereafter state switching is repeatable.

B. Pull-off Force

Next, we investigated the pull-off forces of the compliant magnets, including the pull-off forces of the EP magnets in both ON and OFF states. The same samples from Section IV-A were magnetized with a self-contained magnetizer (MAG24C; Master Magnetics) and then adhered to 6.35 mm-thick acrylic plates with a silicone adhesive (Sil-Poxy; Smooth-On). Samples were then brought in contact with a 76.2 mm x 76.2 mm A36 low-carbon steel plate (1388K102; McMaster-Carr) with a thickness of 6.35 mm. The sample was compressed by the steel plate at a rate of 3 mm/min until a compressive force of 50 mN was measured by the load cell. We note that the 50 mN threshold represents a coupled measurement between the compression force and the force of magnetic attraction, and samples with different stiffnesses will experience different compressive strains at 50 mN, yet some normalizing threshold must be chosen. After the initial normalizing compression, the plate was pulled off the sample at a rate of 3 mm/min, and the peak magnetic pull-off force was measured. The results for five samples of each weight percent and material are shown in Figure 5. Congruent with the results from Figure 3, the NdFeB samples exert higher forces than the AlNiCo samples due to NdFeB's greater remanence. Samples with higher weight percents exert stronger forces due to the greater magnetic moments that come from higher magnetic volumes. The results also demonstrate that, to achieve the desired properties of electropermanence in our EP samples, we compromise on the strength of our magnets compared to NdFeB composites.

The same pull-off experiments were repeated on the EP

samples after toggling the state from ON to OFF and vice versa. The state of the EP magnet can be switched by subjecting it to a magnetic field antiparallel to its magnetization if that field is sufficiently above the coercivity of AlNiCo but well below the coercivity of NdFeB. In practice, we used a 10 mm coil made from 400 turns of 24 AWG enameled copper wire (7588K77; McMaster-Carr) energized with 10 A of current. The coil has an inner radius of 15 mm, and when energized, it produces a magnetic field with a maximum magnitude of 400 kA/m (0.5 T) along its central axis per Equation 1:

$$H = \frac{NI}{l} \quad (1)$$

where H is the applied field, N is the number of turns, I is the current, and l is the overall length of the coil. To switch the state from ON to OFF, the EP sample is placed in the center of the coil and held in place such that the field produced by the coil will be antiparallel to its magnetization. Then, the coil is energized with a brief (>1 ms) pulse of current. We know from previous literature [19], [25] that electropermanent magnets saturate if the pulse duration is at least 1 ms, so any pulse >1 ms should yield the same result. To switch the state from OFF to ON, this procedure is repeated with the sample flipped relative to the coil.

Figure 6 shows the results of the pull-off force experiment for five EP samples of each weight percent. There is a large decrease in pull-off force compared to the initial magnetization after switching the EP magnets OFF and then ON again because we do not use a saturating field (2,400 kA/m) to switch states, but rather a much weaker field (≤ 400 kA/m). After the first cycle, the ON and OFF states demonstrate stable switching, with the difference between states more pronounced at higher weight percents. Even in the OFF state, the samples still have some remanent magnetization, so the pull-off forces are nonzero; however, they are weaker than the forces in the ON state, and in practice that discrepancy makes the difference in the 80% sample's ability to hold its own weight (see Section V).

V. DEMONSTRATION OF THE COMPLIANT ELECTROPERMANENT MAGNET

Figure 7 and the supplementary video illustrate the operational principle of compliant electropermanent magnets. Compliant electropermanent magnets exhibit the mechanical compliance necessary to be integrated into the bodies of soft robots. Furthermore, their magnetism can be turned ON and OFF with a brief pulse of a magnetic field of 400 kA/m. In the supplementary video, a newly magnetized compliant electropermanent magnet (80% EP, identical to the samples from Section IV) is shown lifting a paper clip with a mass of 0.5 g and supporting its own weight with its magnetism in the presence of a ferromagnetic surface, in this case, needle-nose pliers. Then, the compliant electropermanent magnet is held in place by a piece of tape in the center of an electromagnetic coil (400 turns of 24 AWG wire as in Section IV) that is briefly (>1 ms) energized with 10 A of current. The induced

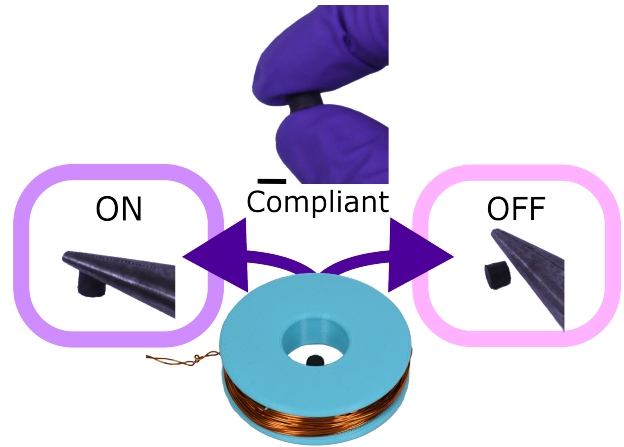


Fig. 7. Operating principle of the compliant electropermanent magnet. The material is compliant, so it can be easily compressed. The scale bar is 6 mm. When in the ON state, it can support its own weight magnetically, as shown, as it is lifted by a pair of pliers. In the OFF state, it cannot. The state can be switched by placing the compliant electropermanent magnet in a magnetic field of about 400 kA/m, for example, in the hand-made electromagnetic coil shown. The reader is directed to the supplementary video to see the state switching demonstrated.

magnetic field is strong enough to reverse the polarity of the AlNiCo in the EP magnet but not strong enough to affect the NdFeB, resulting in a net magnetization close to zero (the OFF state). Once turned OFF, the compliant electropermanent magnet is unable to lift its own weight when in contact with the same pair of pliers, and it struggles to lift the same paper clip. By flipping the coil and placing the compliant electropermanent magnet in its center once more, the magnet is turned back ON, and it again can easily lift the paper clip and support its own weight, sticking to the pliers via magnetism. Note that the magnetic force is dependent on the object the magnet attaches to, and the paper clip used in this demonstration has a much smaller ferromagnetic volume than the steel plate from Section IV.

The process of turning the compliant electropermanent magnet ON and OFF is reversible and repeatable. These compliant magnets can be used in soft robots that would benefit from the ability to selectively magnetize parts of their compliant bodies.

VI. CONCLUSION

This paper introduced the compliant electropermanent magnet, a mechanically compliant material whose permanent magnetism can be switched ON and OFF by subjecting it to a magnetic field. We illustrated the process for designing compliant electropermanent magnets by measuring the remanent magnetization and coercivity of magnetic powders and selecting mixing ratios to achieve desired properties. Experiments characterized the mechanical compliance of this material and the forces it can generate. Lastly, we demonstrated the repeatable, reversible switching between ON and OFF states.

Future work can incorporate different magnetic materials and mixing ratios to expand the design space and enable further tunability in magnetic soft robots. A limitation of

this work is the necessity of a rigid, external coil in contrast to the co-located coils in rigid electropermanent magnets; further advances in compliant electromagnetic coils that can achieve high field strengths would complement this work. Finally, future research can focus on integrating compliant electropermanent magnets into the bodies of soft robots to evaluate their efficacy in robotics applications.

ACKNOWLEDGMENT

The authors thank Peter Schiffer for providing access to the SQUID MPMS 3 and Ioan-Augustin Chioar for conducting the VSM experiments in Section III.

REFERENCES

- [1] D. Rus and M. T. Tolley, "Design, fabrication and control of soft robots," *Nature*, vol. 521, no. 7553, pp. 467–475, 2015.
- [2] W. R. Johnson, A. Agrawala, X. Huang, J. Booth, and R. Kramer-Bottiglio, "Sensor tendons for soft robot shape estimation," in *2022 IEEE Sensors*. IEEE, 2022, pp. 1–4.
- [3] J. Shintake, E. Piskarev, S. H. Jeong, and D. Floreano, "Ultrastretchable strain sensors using carbon black-filled elastomer composites and comparison of capacitive versus resistive sensors," *Advanced Materials Technologies*, vol. 3, no. 3, p. 1700284, 2018.
- [4] X. Huang, K. Kumar, M. K. Jawed, A. Mohammadi Nasab, Z. Ye, W. Shan, and C. Majidi, "Highly dynamic shape memory alloy actuator for fast moving soft robots," *Advanced Materials Technologies*, vol. 4, no. 4, p. 1800540, 2019.
- [5] D. J. Preston, P. Rothemund, H. J. Jiang, M. P. Nemitz, J. Rawson, Z. Suo, and G. M. Whitesides, "Digital logic for soft devices," *Proceedings of the National Academy of Sciences*, vol. 116, no. 16, pp. 7750–7759, 2019.
- [6] M. Mohammadi, M. Berggren, and K. Tybrandt, "Versatile ultra-soft electromagnetic actuators with integrated strain-sensing cellulose nanofibril foams," *Advanced Intelligent Systems*, p. 2200449, 2023.
- [7] W. R. Johnson, S. J. Woodman, and R. Kramer-Bottiglio, "An electromagnetic soft robot that carries its own magnet," in *2022 IEEE 5th International Conference on Soft Robotics (RoboSoft)*. IEEE, 2022, pp. 761–766.
- [8] G. Mao, M. Drack, M. Karami-Mosammam, D. Wirthl, T. Stockinger, R. Schwödauer, and M. Kaltenbrunner, "Soft electromagnetic actuators," *Science advances*, vol. 6, no. 26, p. eabc0251, 2020.
- [9] W. Hu, G. Z. Lum, M. Mastrangeli, and M. Sitti, "Small-scale soft-bodied robot with multimodal locomotion," *Nature*, vol. 554, no. 7690, pp. 81–85, 2018.
- [10] L. S. Novelino, Q. Ze, S. Wu, G. H. Paulino, and R. Zhao, "Untethered control of functional origami microrobots with distributed actuation," *Proceedings of the National Academy of Sciences*, vol. 117, no. 39, pp. 24 096–24 101, 2020.
- [11] P. Lloyd, T. L. Thomas, V. K. Venkiteswaran, G. Pittiglio, J. H. Chandler, P. Valdastrì, and S. Misra, "A magnetically-actuated coiling soft robot with variable stiffness," *IEEE Robotics and Automation Letters*, vol. 8, no. 6, pp. 3262–3269, 2023.
- [12] M. Richter, M. Kaya, J. Sikorski, L. Abelman, V. Kalpathy Venkiteswaran, and S. Misra, "Magnetic soft helical manipulators with local dipole interactions for flexibility and forces," *Soft Robotics*, vol. 10, no. 3, pp. 647–659, 2023.
- [13] N. Kohls, B. Dias, Y. Mensah, B. P. Ruddy, and Y. C. Mazumdar, "Compliant electromagnetic actuator architecture for soft robotics," in *2020 IEEE International Conference on Robotics and Automation (ICRA)*. IEEE, 2020, pp. 9042–9049.
- [14] M. Richter, J. Sikorski, P. Makushko, Y. Zabala, V. K. Venkiteswaran, D. Makarov, and S. Misra, "Locally addressable energy efficient actuation of magnetic soft actuator array systems," *Advanced Science*, p. 2302077, 2023.
- [15] N. Kohls, I. Abdeally, B. P. Ruddy, and Y. C. Mazumdar, "Design of a xenia coral robot using a high-stroke compliant linear electromagnetic actuator," *ASME Letters in Dynamic Systems and Control*, vol. 1, no. 3, p. 031011, 2021.
- [16] N. D. Kohls, R. Balak, B. P. Ruddy, and Y. C. Mazumdar, "Soft electromagnetic motor and soft magnetic sensors for synchronous rotary motion," *Soft Robotics*, 2023.
- [17] M. Li, A. Pal, J. Byun, G. Gardi, and M. Sitti, "Magnetic putty as a reconfigurable, recyclable, and accessible soft robotic material," *Advanced Materials*, p. 2304825, 2023.
- [18] K. Gilpin, A. Knaian, and D. Rus, "Robot pebbles: One centimeter modules for programmable matter through self-disassembly," in *2010 IEEE International Conference on Robotics and Automation*. IEEE, 2010, pp. 2485–2492.
- [19] A. N. Knaian, "Electropermanent magnetic connectors and actuators: devices and their application in programmable matter," Ph.D. dissertation, Massachusetts Institute of Technology, 2010.
- [20] J. Daudelin, G. Jing, T. Tosun, M. Yim, H. Kress-Gazit, and M. Campbell, "An integrated system for perception-driven autonomy with modular robots," *Science Robotics*, vol. 3, no. 23, p. eaat4983, 2018.
- [21] T. Tosun, J. Davey, C. Liu, and M. Yim, "Design and characterization of the ep-face connector," in *2016 IEEE/RSJ International Conference on Intelligent Robots and Systems (IROS)*. IEEE, 2016, pp. 45–51.
- [22] G. Jing, T. Tosun, M. Yim, and H. Kress-Gazit, "An end-to-end system for accomplishing tasks with modular robots," in *Robotics: Science and systems*, vol. 2, 2016, p. 7.
- [23] S. Hong, Y. Um, J. Park, and H.-W. Park, "Agile and versatile climbing on ferromagnetic surfaces with a quadrupedal robot," *Science Robotics*, vol. 7, no. 73, p. eadd1017, 2022.
- [24] A. D. Marchese, C. D. Onal, and D. Rus, "Soft robot actuators using energy-efficient valves controlled by electropermanent magnets," in *2011 IEEE/RSJ International Conference on Intelligent Robots and Systems*. IEEE, 2011, pp. 756–761.
- [25] K. J. McDonald, L. Kinnicutt, A. M. Moran, and T. Ranzani, "Modulation of magnetorheological fluid flow in soft robots using electropermanent magnets," *IEEE Robotics and Automation Letters*, vol. 7, no. 2, pp. 3914–3921, 2022.
- [26] P. Zhang, M. Kamezaki, Z. He, H. Sakamoto, and S. Sugano, "Epm-mre: electropermanent magnet-magnetorheological elastomer for soft actuation system and its application to robotic grasping," *IEEE Robotics and Automation Letters*, vol. 6, no. 4, pp. 8181–8188, 2021.
- [27] C. Zhang, P. Zhu, Y. Lin, Z. Jiao, and J. Zou, "Modular soft robotics: Modular units, connection mechanisms, and applications," *Advanced Intelligent Systems*, vol. 2, no. 6, p. 1900166, 2020.
- [28] J.-Y. Lee and K.-J. Cho, "Development of magnet connection of modular units for soft robotics," in *2017 14th International Conference on Ubiquitous Robots and Ambient Intelligence (URAI)*. IEEE, 2017, pp. 65–67.
- [29] A. Vergara, Y.-s. Lau, R.-F. Mendoza-Garcia, and J. C. Zagal, "Soft modular robotic cubes: toward replicating morphogenetic movements of the embryo," *PLoS one*, vol. 12, no. 1, p. e0169179, 2017.
- [30] W. Wang, N.-G. Kim, H. Rodrigue, and S.-H. Ahn, "Modular assembly of soft deployable structures and robots," *Materials horizons*, vol. 4, no. 3, pp. 367–376, 2017.
- [31] J. Zou, Y. Lin, C. Ji, and H. Yang, "A reconfigurable omnidirectional soft robot based on caterpillar locomotion," *Soft robotics*, vol. 5, no. 2, pp. 164–174, 2018.
- [32] L. Zhao, Y. Wu, J. Blanchet, M. Perroni-Scharf, X. Huang, J. Booth, R. Kramer-Bottiglio, and D. Balkcom, "Soft lattice modules that behave independently and collectively," *IEEE Robotics and Automation Letters*, vol. 7, no. 3, pp. 5942–5949, 2022.
- [33] L. Zhao, Y. Wu, W. Yan, W. Zhan, X. Huang, J. Booth, A. Mehta, K. Bekris, R. Kramer-Bottiglio, and D. Balkcom, "Starblocks: Soft actuated self-connecting blocks for building deformable lattice structures," *IEEE Robotics and Automation Letters*, 2023.
- [34] L. Wang and F. Iida, "Towards 'soft' self-reconfigurable robots," in *2012 4th IEEE RAS & EMBS International Conference on Biomedical Robotics and Biomechanics (BioRob)*. IEEE, 2012, pp. 593–598.
- [35] G. Park and H. Rodrigue, "Soft climbing robot with magnetic feet for multimodal locomotion," *Scientific Reports*, vol. 13, no. 1, p. 8377, 2023.